Robust Carrier Frequency Offset Estimation with Reduced Overhead for Coherent Optical OFDM Systems

David Rörich[1], Ivan Vaklinov[2], Stephan ten Brink[3]
Universität Stuttgart, Institut für Nachrichtenübertragung
[1]roerich@inue.uni-stuttgart.de, [2]i_d_v@abv.bg, [3]tenbrink@inue.uni-stuttgart.de

Abstract

We study carrier frequency offset estimation (FOE) and compensation for coherent optical orthogonal frequency division multiplexing (CO-OFDM) systems. A robust FOE is crucial for OFDM reception as multicarrier systems are particularly susceptible to frequency offset. We present an FOE algorithm that reduces training overhead by exploiting the pilot symbols used for channel estimation instead of dedicated FOE pilot symbols. Our simulations show that the proposed algorithm is robust against noise and dispersion over a wide range of frequency offsets. Additionally, the impact of random laser phase walk on system performance and estimation error is examined.

1 Introduction

CO-OFDM is considered a promising modulation scheme for high-capacity optical communications with bit rates towards 400 Gbit/s per wavelength [1]. Recent advances in the real-time implementation of CO-OFDM systems have shown that this transmission scheme is a realistic option for future high-speed and flexible optical networks [2]–[5]. While CO-OFDM enables software-defined bandwidth and bit rate allocation, and while it has been demonstrated to be resilient to chromatic dispersion (CD), it is also known to be susceptible to carrier frequency offset (CFO) which causes inter-carrier interference. Hence, robust FOE and compensation is an important aspect of every CO-OFDM receiver.

In principle, FOE methods can be divided into two categories: (1) data-aided and blind methods based on digital signal processing (DSP) and (2) methods based on tracking an optical pilot carrier. Techniques from the latter category can deliver an accurate FOE [6] and phase noise estimation [7], but require a higher receiver dynamic range or an additional guard band reducing the bit rate [8]. Methods in category (1) avoid these issues but generally have a higher computational complexity and often rely on the insertion of special pilot symbols thus introducing additional overhead [9], [10]. In this work we present a DSP-based FOE method with excellent robustness against noise and CD that exploits the pilot symbols used for channel estimation and thus avoids additional overhead.

This paper is organized as follows. In section 2 the system model used for numerical simulations and the transmission frame structure are presented. Section 3 gives a detailed description of the proposed FOE algorithm and discusses a method for estimating the residual frequency offset as well as the random laser phase walk. Simulation results of the proposed method are compared with an existing method in section 4; section 5 concludes the paper.

2 System model

The CO-OFDM system considered in this work employs two free-running laser sources and is shown in **Fig. 1**. The transmit laser generates the optical

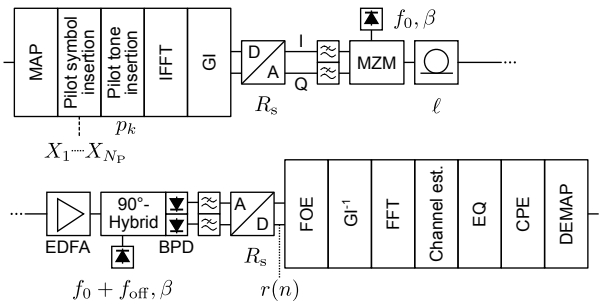

Figure 1 Block diagram of the CO-OFDM system.

carrier with frequency f_0 from which the frequency of the receive laser deviates by f_{off}. Both lasers exhibit the same linewidth β. At the transmitter input the incoming bit sequence is mapped onto complex symbols, where the symbol alphabet can be a quadrature amplitude modulation (QAM) constellation with 4, 16, 64 or 256 symbols. The system uses N subcarriers and the OFDM modulation is realized by an N-point inverse fast Fourier transform (IFFT). In this work, we chose $N = 256$, where 86 subcarriers at the spectrum margins are left unmodulated to faciliate anti-aliasing filtering at the receiver. After inserting the guard interval (GI), which is a cyclic repetition

of N_G samples of the time-domain OFDM symbol, the complex discrete-time signal is converted to the inphase (I) and quadrature (Q) analog signals at a rate of R_s samples per second. Amplitude and phase of the optical carrier are modulated by the I and Q signals driving two nested Mach-Zehnder modulators (MZMs) whose non-linear characteristic is neglected assuming that the modulation index is kept sufficiently low [11]. The MZM output is fed into a standard single mode fiber (SSMF) of length ℓ with a chromatic dispersion coefficient of 17 ps/(nm km). Although not implemented in our system model, we assume that the state of polarization can be tracked using a polarization diverse receiver and DSP, which is why polarization mode dispersion (PMD) is neglected here. Additionally, fiber nonlinearities are not taken into account under the assumption that the optical launch power is sufficiently low. The received signal is amplified by an erbium doped fiber amplifier (EDFA) which is modelled by the addition of white Gaussian noise. The amplified signal is then mixed with the receive laser in a 90° hybrid for optical downconversion and detected with two balanced photodiodes (BPDs). After analog-to-digital conversion with sampling rate $R_\mathrm{s} = 32\,\mathrm{GBd}$ the FOE is executed (see section 3). Subsequently, the GI is removed and the received signal is transformed to frequency domain using an N-point FFT. After channel estimation (CE) and equalization (EQ), the effect of laser phase noise is mitigated by estimating and compensating the common phase error (CPE) using the pilot tones p_k inserted at the transmitter (see section 3.3). Finally, symbol decision is performed in the demapper (DEMAP) and the received symbols are converted back to a bit sequence which is compared to the transmitted bits yielding the bit error rate (BER).

The transmitted data are structured in transmission frames starting with N_P pilot symbols $X_1, \ldots, X_{N_\mathrm{P}}$ followed by N_D payload OFDM symbols. By dividing the received pilot symbols by the known transmitted pilot symbols the channel transfer function is estimated, while averaging over N_P estimations reduces the impact of noise on the CE as previously shown in [12]. The choice of N_P is therefore determined by the tolerable optical signal-to-noise ratio (OSNR) that is required to reach a sufficiently low BER before forward error correction. As a conservative limit for this minimum BER we chose 10^{-3}. Due to imperfect CE there is a penalty compared to a system with perfect channel knowledge. **Fig. 2** shows simulation results of this OSNR penalty as a function of N_P for different modulation orders. It is found that the OSNR penalty initially decreases steeply and then saturates for large numbers of N_P. In this work, $N_\mathrm{P} = 10$ was chosen as a compromise between overhead and OSNR penalty. In order to track changes of the channel transfer function the CE is repeated every N_D OFDM symbols corresponding to an update period $T_\mathrm{U} = N_\mathrm{D} T_\mathrm{s}$, where

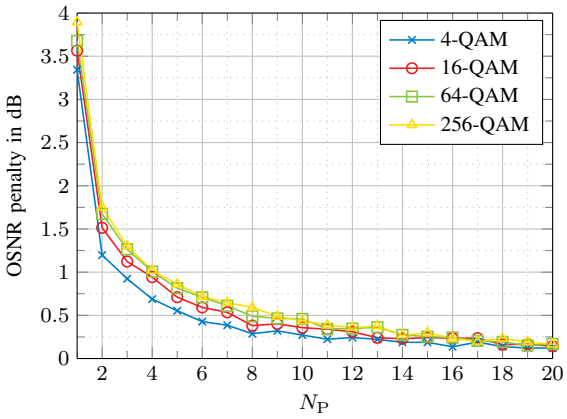

Figure 2 OSNR penalty due to imperfect CE as a function of N_P for different modulation orders.

$T_\mathrm{s} = (N + N_\mathrm{G})/R_\mathrm{s}$ is the OFDM symbol duration. While the chromatic dispersion coefficient of a single mode fiber varies slowly, field measurements have revealed that the state of polarization can change in less than a millisecond [13], [14]. Accordingly, $T_\mathrm{U} \ll 1\,\mathrm{ms}$ should hold and is chosen to be 20 µs here. Depending on the fiber length, N_G varies and consequently the maximum value of N_D depends on the transmission scenario. Here, it is fixed to $N_\mathrm{D} = 2000$. The pilot symbols for CE can in principle be arbitrary 4-QAM OFDM symbols [12], [15]. Motivated by the FOE algorithm we chose the first $N_\mathrm{P} - 1$ pilot symbols to be identical, while the last pilot symbol is different. In the following section it will be discussed how this frame structure can be useful for FOE.

3 FOE algorithm

The presented FOE algorithm is based on a concept introduced by Schmidl and Cox in [10]. They proposed to generate a special OFDM pilot symbol with a repetitive structure in time domain by setting every second subcarrier of that pilot symbol to zero. This results in an OFDM symbol with two identical halves in time domain. Our method also relies on a repetitive time domain structure but does not presume any special frequency domain structure. Instead, it exploits the repetition of identical pilot symbols at the beginning of a frame. By comparing the received phase of two samples with known distance and identical transmit value the frequency offset can be estimated through the observed phase change. A detailed explanation of this estimation is given in section 3.1. Due to phase ambiguities the estimation range of this step is limited and generally has to be extended by another step which is presented in section 3.2. In section 3.3 a technique that compensates for the residual frequency offset is discussed.

3.1 Fractional FOE

The received and sampled signal $r(n)$ can be written as

$$r(n) = y(n)\mathrm{e}^{\mathrm{j}\left(2\pi\frac{f_{\mathrm{off}}}{R_{\mathrm{s}}}n+\phi(n)\right)} + w(n), \quad (1)$$

where n is the discrete time, $y(n) = x(n) * h(n)$ is the transmitted signal $x(n)$ convolved with the channel impulse response $h(n)$, and $\phi(n)$ is the random laser phase. The noise term $w(n)$ follows a Gaussian distribution with zero mean. As can be seen from (1), the frequency offset f_{off} between transmit and receive laser causes a linear phase rotation of the received signal. In order to estimate this phase rotation we evaluate the following correlation sum:

$$R(n_0) = \sum_{l=0}^{N+N_{\mathrm{G}}-1} r^*(n_0+l)r(n_0+l+N+N_{\mathrm{G}}), \quad (2)$$

where n_0 represents the discrete time index of the beginning of a frame. We recall the frame structure that starts with N_{P} pilot symbols of which the first $N_{\mathrm{P}}-1$ are identical. Thus, for the transmitted signal $x(n_0) = x(n_0+N+N_{\mathrm{G}})$ holds. If the guard interval is at least as long as the channel delay spread it follows that $y(n_0) = y(n_0+N+N_{\mathrm{G}})$ and neglecting the noise terms $w(n), \phi(n)$ we can rewrite (2):

$$R(n_0) = \mathrm{e}^{\mathrm{j}2\pi\frac{f_{\mathrm{off}}}{R_{\mathrm{s}}}(N+N_{\mathrm{G}})} \sum_{l=0}^{N+N_{\mathrm{G}}-1} |y(n_0+l)|^2. \quad (3)$$

The frequency offset could now be estimated by evaluating the phase of $R(n_0)$ in (3). $R(n_0)$ takes the first two pilot symbols into account, but as the frame start contains $N_{\mathrm{P}}-1$ identical pilot symbols we can extend (3) by correlating every pair of neighboring pilot symbols yielding

$$Q(n_0) = \sum_{i=0}^{N_{\mathrm{P}}-3} R\left(n_0 + i(N+N_{\mathrm{G}})\right). \quad (4)$$

Finally, the frequency offset estimation is calculated by

$$\hat{f}_{\mathrm{I}} = \frac{R_{\mathrm{s}}}{2\pi(N+N_{\mathrm{G}})} \cdot \mathrm{arc}\{Q(n_0)\}, \quad (5)$$

where $\mathrm{arc}(a) \in [-\pi, \pi]$ is the phase angle of a. It follows from that phase ambiguity that the estimation range of $\hat{f}_{\mathrm{I}}$ is limited to

$$\left|\hat{f}_{\mathrm{I}}\right| \leq \frac{R_{\mathrm{s}}}{2(N+N_{\mathrm{G}})}. \quad (6)$$

After estimation of f_{I}, the frequency offset is removed by reversing the linear phase rotation:

$$\tilde{r}_{\mathrm{I}}(n) = r(n)\exp\left(-\mathrm{j}2\pi(\hat{f}_{\mathrm{I}}/R_{\mathrm{s}})n\right). \quad (7)$$

If f_{off} exceeds the range defined in (6) there will be a remaining frequency offset of $f_{\mathrm{II}} = (MR_{\mathrm{s}})/(N+N_{\mathrm{G}})$. As M is an integer number this frequency offset is referred to as integer frequency offset, while f_{I} is denoted fractional frequency offset. As a consequence of the typically long symbol durations encountered in OFDM the estimation range of $\hat{f}_{\mathrm{I}}$ is relatively small and usually lies in the order of tens to hundreds of Megahertz for practical CO-OFDM systems. In the system considered here, for example $R_{\mathrm{s}} = 32\,\mathrm{GBd}$, $N = 256$, and $N_{\mathrm{G}} = 8$ which yields an estimation range of $|\hat{f}_{\mathrm{I}}| \leq 60.6\,\mathrm{MHz}$. In contrast, commercially available laser sources exhibit a frequency accuracy of about 2.5 GHz, so that the frequency offset can be as large as 5 GHz. Therefore, f_{II} has to be estimated in addition to estimating f_{I}, which will be discussed in the following section.

3.2 Integer FOE

The problem of estimating the integer frequency offset f_{II} can be solved by searching the value of M that maximizes the correlation of the received pilot symbol with a frequency shifted version of the transmitted pilot symbol in frequency domain [10]. As discussed in section 3.1 practical values of f_{off} are limited and thus the search of M can be restricted to a range $[-\bar{M}, \bar{M}]$. Since the OFDM receiver exhibits an N-FFT to demodulate the received signal after guard interval removal it is beneficial for this method to have a frequency shift which is an integer multiple of R_{s}/N. This is because the received signal will be compared with frequency shifted versions of the transmitted signal which, by using an N-IDFT, exhibits a subcarrier spacing R_{s}/N. Therefore, the received signal is first frequency shifted, so that it matches the frequency spacing of an N-point discrete Fourier transform (DFT):

$$z(n, M) = \tilde{r}_{\mathrm{I}}(n)\exp\left(\mathrm{j}2\pi M\left(\frac{1}{N} - \frac{1}{N+N_{\mathrm{G}}}\right)n\right). \quad (8)$$

Let $X_1(k)$ and $X_{N_{\mathrm{P}}}(k)$ be the frequency-domain representation of the first and last transmitted pilot symbol of a frame, respectively. Accordingly, $Z_1(k, M)$ and $Z_{N_{\mathrm{P}}}(k, M)$ are the N-DFTs of the subsets of $z(n, M)$ that represent the first and last received pilot symbol (excluding guard interval). The correlation sum to be maximized is then defined as

$$S(M) = \left|\sum_{k=0}^{N-1} Z_1^*(k, M)\frac{X_{N_{\mathrm{P}}}^*(k-M)}{X_1^*(k-M)}Z_{N_{\mathrm{P}}}(k, M)\right|^2. \quad (9)$$

If M corresponds to the actual integer frequency offset, the argument of the above sum becomes real-valued and the estimation of M can thus be found by

$$\hat{M} = \underset{M\in[-\bar{M},\bar{M}]}{\arg\max}\, S(M). \quad (10)$$

Subsequently, the estimation of the integer frequency offset is computed by

$$\hat{f}_{\mathrm{II}} = \hat{M}\frac{R_{\mathrm{s}}}{N+N_{\mathrm{G}}} \quad (11)$$

and the total frequency offset estimation is given by

$$\hat{f}_{\text{off}} = \hat{f}_{\text{I}} + \hat{f}_{\text{II}}. \tag{12}$$

It should be noted that even small estimation errors $f_{\text{e}} = f_{\text{off}} - \hat{f}_{\text{off}}$ can have considerable impact on the received constellation diagram and thus on the BER. Consider an actual frequency offset of 1 GHz and an estimation error of $f_{\text{e}}/f_{\text{off}} = 0.1\%$. With $R_{\text{s}} = 32\,\text{GBd}$, $N = 256$, and $N_{\text{G}} = 8$ the residual frequency offset leads to a 90° phase shift during 30 OFDM symbols making correct symbol decision at the receiver virtually impossible. Consequently, a method to track this slow but eventually harmful phase rotation has to be found and will be discussed in the following section.

3.3 Common phase error estimation

The phase rotation caused by the residual frequency offset f_{e} is $2\pi(f_{\text{e}}/R_{\text{s}})n$. As $f_{\text{e}} \ll R_{\text{s}}$ the phase rotation during one OFDM symbol, which consists of $N + N_{\text{G}}$ samples, can be considered to be approximately constant. This assumption can also be made for the phase error induced by random laser phase walk [16], so that every OFDM symbol is affected by a CPE ϕ_{e} combining phase noise and residual frequency offset. This CPE has to be estimated for all OFDM symbols individually. One way to do so is to use L subcarriers as pilot tones which are modulated with known complex values p_k. The CPE of an OFDM symbol can then be estimated by

$$\hat{\phi}_{\text{e}} = \arc\left(\sum_{k=0}^{L-1} \tilde{p}_k p_k^*\right), \tag{13}$$

where $\tilde{p}_k$ is the received value of the kth pilot tone after equalization. Let $\phi(t)$ be the combined phase noise of transmit and receiver laser. Then the effective laser phase $\psi(t)$ after CFO compensation can be thought of as $\psi(t) = 2\pi f_{\text{e}} t + \phi(t)$. **Fig. 3** shows the simulated phase $\psi(t)$ for $\beta = 100\,\text{kHz}$, $f_{\text{off}} = 0\,\text{Hz}$ and

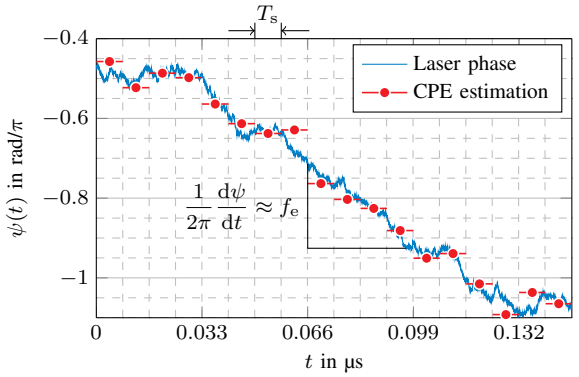

Figure 3 Combined laser phase $\psi(t)$ and CPE estimations for $\beta = 100\,\text{kHz}$, $f_{\text{e}} = -2.2\,\text{MHz}$, $\ell = 80\,\text{km}$ and $L = 6$ at an OSNR of 15 dB.

$f_{\text{e}} = -2.2\,\text{MHz}$. The residual frequency offset causes a linear phase decline which is overlaid with random phase fluctuations. The CPE estimations are indicated in Fig. 3 by horizontal lines spanning the duration of one OFDM symbol of length $T_{\text{s}} = 8.25\,\text{ns}$.

It is worth noting that the calculation of $\hat{f}_{\text{II}}$ is computationally demanding as it requires the calculation of $2\bar{M} + 1$ N-DFTs. However, the frequency of common laser sources changes very slowly compared to the repetition rate of the pilot symbols: The laser frequency drift lies in the order of hundreds of Megahertz per hour [5], [17], whereas pilot symbols should be transmitted several thousand times per second to follow fast polarization state changes as discussed earlier. It is therefore sufficient to execute an initial estimation of $\hat{f}_{\text{II}}$ during an acquisition phase and to track the frequency offset using only the fractional FOE $\hat{f}_{\text{I}}$ thereafter. During the acquisition phase the N-FFT block else performing data demodulation can be used.

4 Results and discussion

In order to evaluate the proposed FOE algorithm we conducted computer simulations of the system described in section 2. To study the accuracy of the FOE the mean squared error (MSE) of the estimation was calculated by

$$\frac{1}{N_{\text{E}}} \sum_{i=1}^{N_{\text{E}}} \left(\frac{f_{\text{off}} - \hat{f}_{\text{off},i}}{R_{\text{s}}/N}\right)^2, \tag{14}$$

where N_{E} is the number of estimations. All MSE values presented in the following are based on $N_{\text{E}} = 1000$ estimations. In **Fig. 4** the MSE of the proposed algorithm (PLT) and of the estimation method of Schmidl and Cox (SC) in [10] are compared for frequency offsets between 100 kHz and 5 GHz. Additionally, Fig. 4 shows results for different values of β. It is noted that β is the *respective* linewidth of transmit and receive laser, not the combined linewidth. From Fig. 4 it is found that both algorithms have constant performance over a wide range of frequency offsets covering all values to be expected in practical systems. While the theoretical estimation range of the PLT method is $|f_{\text{off}}| < R_{\text{s}}/2$, the practical limit is determined by the signal and receiver bandwidth, as the frequency shift of the received signal might lead to the attenuation of some frequency components by the anti-aliasing filter and other electrical components with a low-pass characteristic. Fig. 4 also reveals that the proposed algorithm exhibits a much lower MSE than the SC method. This is expected since the PLT method is based on a greater number of correlation pairs than the SC method, namely $(N_{\text{P}} - 2)(N + N_{\text{G}})$ compared to $N/2$. Both methods show a decreasing performance for increasing linewidth as the CPE compensation is

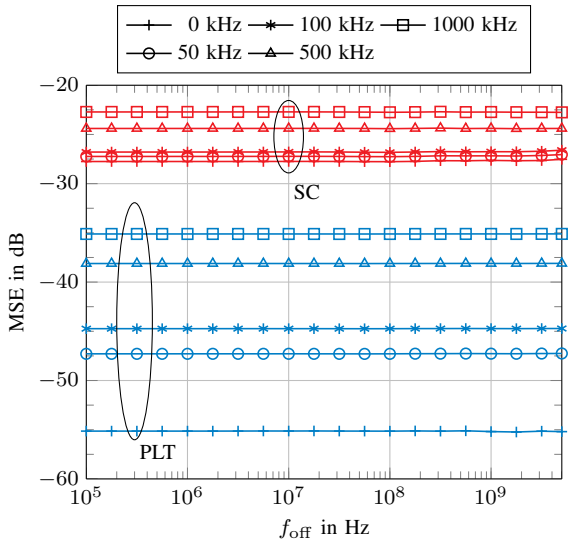

Figure 4 Comparison of the MSE of the PLT and SC method as a function of frequency offset for different linewidths at an OSNR of 6 dB and with $\ell = 80\,\text{km}$.

executed after the FOE which consequently suffers from the uncompensated random laser phase walk. The time distance of two correlated samples is $N/2$ for the SC method and $N+N_\text{G}$ for the PLT method. Therefore, the SC method shows a higher tolerance towards the random laser phase walk, because the random phase change between two correlated samples is statistically smaller than for the PLT method.

In **Fig. 5** the MSE of both methods is shown as a function of OSNR. For $\beta = 0\,\text{kHz}$ the MSE decreases

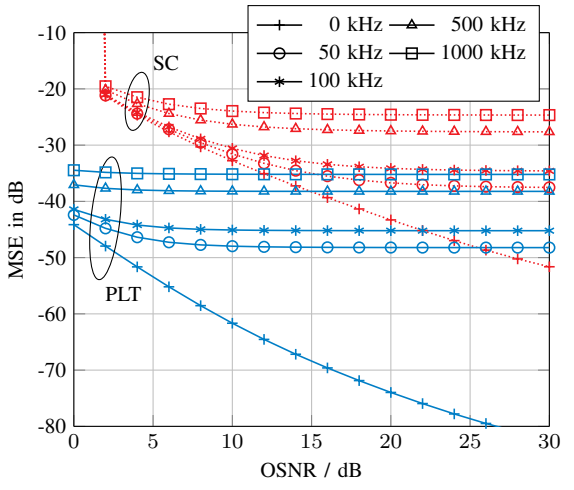

Figure 5 Comparison of the MSE of the PLT and SC method as a function of OSNR for different linewidths, with $\ell = 80\,\text{km}$ and $f_\text{off} = 1\,\text{GHz}$.

with increasing OSNR. However for $\beta > 0\,\text{kHz}$, the linewidth obviously dominates the MSE which does not improve for larger OSNR values. Although the MSE of the PLT method saturates faster, it still exhibits a lower MSE than the SC method for a given linewidth.

The chromatic dispersion tolerance of the FOE algorithms was examined by simulating the MSE for different fiber lengths ℓ, where N_G was increased proportionally to ℓ. Since $N_\text{P}-1$ neighboring pilot symbols are identical, these pilot symbols experience the same inter-symbol interference and are consequently identical at the fiber output as well. For that reason, the FOE using the PLT method is very robust against chromatic dispersion as can be seen from **Fig. 6**. The

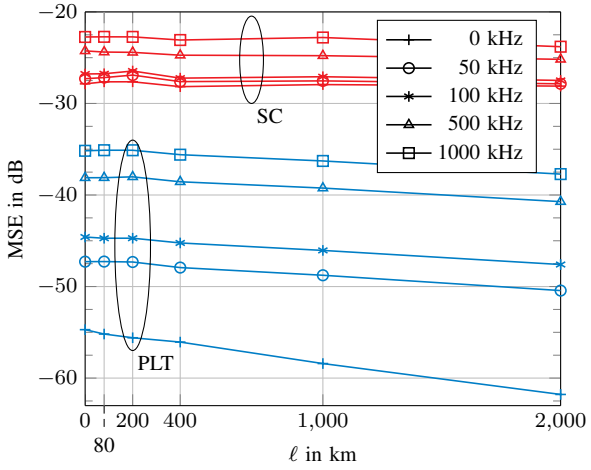

Figure 6 Comparison of the MSE of the PLT and SC method as a function of fiber length for different linewidths at an OSNR of 6 dB and with $f_\text{off} = 1\,\text{GHz}$.

same observation is made for the SC method. The PLT method even improves with increasing fiber length because N_G is increased and subsequently the length of the correlation sum in (2) increases.

For investigating the influence of frequency offset and FOE on the system performance we also determined the required OSNR for a BER of 10^{-3} for various scenarios. **Fig. 7** shows the required OSNR as a function of frequency offset for different modulation orders. In Fig. 7a, the results without random laser phase walk show that the FOE and frequency offset compensation enable nearly penalty-free operation over the complete estimation range. For comparison, the performance of the uncompensated system is given in Fig. 7a as well. It can be observed that the frequency offset tolerance of the uncompensated system decreases for higher modulation orders. Nevertheless, frequency offsets of up to 1 MHz can be compensated for by the CPE estimation described in section 3.3, even without FOE. Furthermore, the PLT method shows a slightly better performance than the SC method for 64- and 256-QAM as shown in the inset of Fig. 7a. In Fig. 7b the required OSNR is shown for a linewidth of 100 kHz. While 4- and 16-QAM exhibit only a small penalty compared to the zero-linewidth case, the performance of the 64-QAM system is severely impaired and a BER of 10^{-3} can only be achieved with the PLT method, albeit with a large penalty of about 8.4 dB.

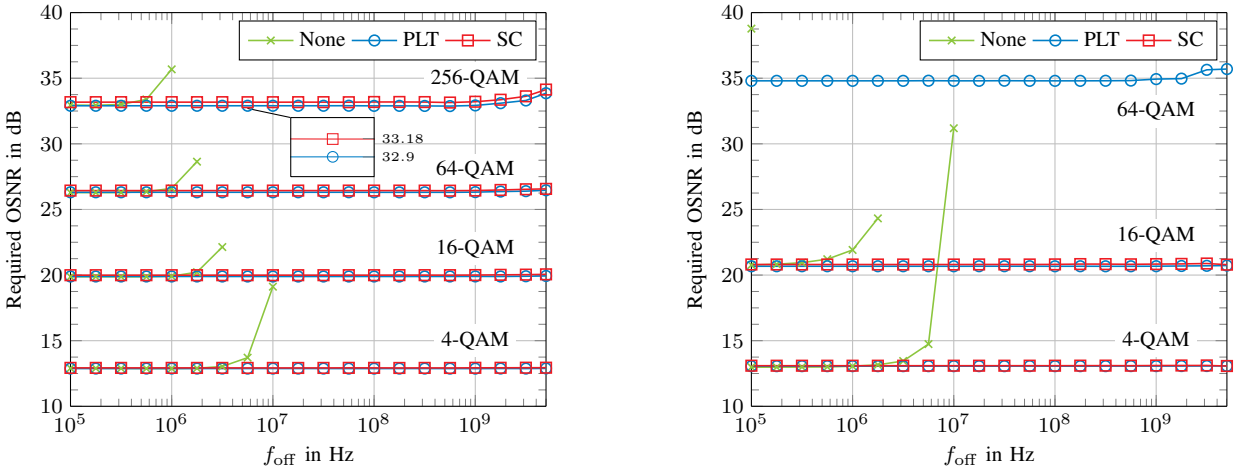

(a) $\beta = 0\,\text{kHz}$ (b) $\beta = 100\,\text{kHz}$

Figure 7 Required OSNR (for BER = 10^{-3}) as a function of frequency offset for different modulation orders, with $\ell = 80\,\text{km}$ and $L = 6$ pilot tones. The required OSNR is plotted for the PLT and SC method, as well as for the system without CFO compensation ("None").

The reception of a 256-QAM OFDM signal was found to be impossible at this linewidth. The influence of laser linewidth on system performance can be studied in more detail in **Fig. 8**, where the required OSNR is plotted as a function of linewidth for different modulation orders and numbers of pilot tones L. Generally,

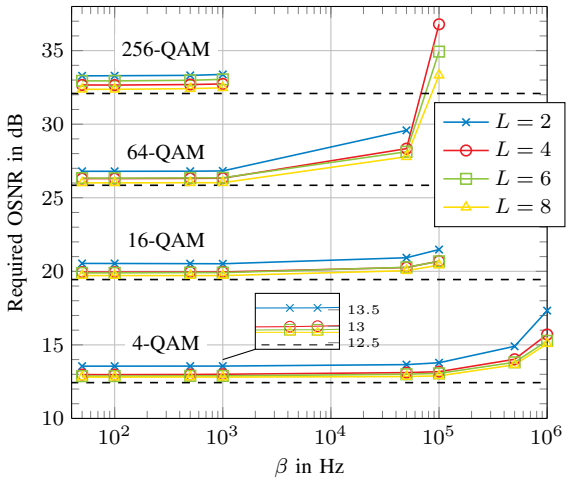

Figure 8 Required OSNR as a function of linewidth for different numbers of pilot tones L with $\ell = 80\,\text{km}$, and $f_{\text{off}} = 1\,\text{GHz}$. Dashed lines indicate the required OSNR of the ideal system.

the required OSNR increases with increasing linewidth, where 4-QAM shows the highest linewidth tolerance. In contrast, 256-QAM reception is found to be feasible only up to $\beta = 1\,\text{kHz}$. It can be seen that the system performance increases only marginally for $L > 4$ and approaches the required OSNR of the ideal system (zero linewidth, no frequency offset) illustrated by the dashed lines in Fig. 8. It is found that the linewidth tolerance cannot be improved substantially by using more pilot tones which indicates that the assumption of a constant phase error during one OFDM symbol is only applicable to moderate linewidths. To improve the linewidth tolerance, advanced CPE methods, which are beyond the scope of this paper, can be employed as described in [18]. For example, the phase error can be tracked on a sub-symbol basis [19]. Alternatively, N can be reduced shortening the symbol duration but at the same time increasing the GI overhead.

As discussed in section 3 the proposed FOE algorithm requires at least two identical pilot symbols and another, third pilot symbol. It is thus more suitable for systems that use long training sequences for CE. In section 2 it has been shown, that in order to reduce the OSNR penalty, rather long training sequences have to be applied. Since the optical channel varies relatively slowly compared to the symbol duration this can be done with moderate overhead. Nevertheless, any overhead reduces the bitrate and should therefore be avoided. The presented method eliminates any FOE overhead and at the same time increases the accuracy and robustness of the FOE as shown by the above results.

5 Conclusion

We have introduced an FOE algorithm based on the method of Schmidl and Cox but tailored for the optical channel with its long coherence time and continuous stream communications. We have shown that the proposed estimation method works for a large range of frequency offsets ($|f_{\text{off}}| \leq 5\,\text{GHz}$) and exhibits superior robustness against noise and dispersive effects. As it exploits the pilot symbols used for channel estimation it also eliminates the need for a special FOE pilot symbol thus reducing the overhead. Although the presented method is more sensitive to random laser phase walk than the SC method, it still achieves a lower MSE for a

given laser linewidth. We have also discussed common phase error estimation as a technique to combat residual frequency offset and random laser phase walk. It is found that the phase noise sensitivity of modulation orders 64- and 256-QAM requires advanced phase estimation techniques which are beyond the scope of this paper. Nevertheless, CO-OFDM systems employing 4- and 16-QAM modulation can be operated at negligible OSNR penalties using 6 pilot tones. Frame synchronization is not covered by this work but it is noted that it can be achieved using the same frame structure as was employed here and will be the subject of future research.

6 Acknowledgment

This work was carried out in the framework of DFG project "Elektronische Schlüsselbausteine für optische OFDM-Systeme hoher Bitrate". The support of DFG is gratefully acknowledged.

References

[1] T. Omiya, M. Yoshida, and M. Nakazawa, "400 Gbit/s 256 QAM-OFDM transmission over 720 km with a 14 bit/s/Hz spectral efficiency by using high-resolution FDE," *Optics Express*, vol. 21, no. 3, pp. 2632–2641, Feb. 2013.

[2] Q. Yang, N. Kaneda, X. Liu, S. Chandrasekhar, W. Shieh, and Y. Chen, "Towards real-time implementation of optical OFDM transmission," in *Optical Fiber Communication Conference*. Optical Society of America, 2010, p. OMS6.

[3] F. Buchali, X. Xiao, S. Chen, and M. Bernhard, "Towards real-time CO-OFDM transceivers," in *Optical Fiber Communication Conference*. Optical Society of America, 2011.

[4] M. Grözing, T. Veigel, H. Huang, J. Briem, J. Zhang, and M. Berroth, "Design of High-Speed Mixed-Signal Circuits in 65 nm and 28 nm CMOS Technology for Optical Transmitters with Data Rates beyond 100 Gbit/s per Wavelength," in *ITG Symposium on Photonic Networks*. Leipzig: VDE Verlag, 2014, pp. 152–155.

[5] N. Kaneda, T. Pfau, H. Zhang, J. Lee, Y.-K. Chen, C. J. Youn, Y. H. Kwon, E. S. Num, and S. Chandrasekhar, "Field demonstration of 100-Gb/s real-time coherent optical OFDM detection," in *European Conference on Optical Communication*, Sep. 2014.

[6] S. Cao, S. Zhang, C. Yu, and P.-Y. Kam, "Full-Range Pilot-Assisted Frequency Offset Estimation for OFDM Systems," in *Optical Fiber Communication Conference*, vol. 1. Washington, D.C.: Optical Society of America, 2013, p. JW2A.53.

[7] S. L. Jansen, I. Morita, N. Takeda, and H. Tanaka, "20-Gb/s OFDM transmission over 4,160-km SSMF enabled by RF-pilot tone phase noise compensation," in *Optical Fiber Communication Conference*. Optical Society of America, 2007, p. PDP15.

[8] Z. Liu, J.-Y. Kim, D. S. Wu, D. J. Richardson, and R. Slavík, "Homodyne OFDM with Optical Injection Locking for Carrier Recovery," *Journal of Lightwave Technology*, vol. 33, no. 1, pp. 34–41, 2015.

[9] P. Moose, "A technique for orthogonal frequency division multiplexing frequency offset correction," *IEEE Transactions on Communications*, vol. 42, no. 10, pp. 2908–2914, 1994.

[10] T. M. Schmidl and D. C. Cox, "Robust frequency and timing synchronization for OFDM," *IEEE Transactions on Communications*, vol. 45, no. 12, pp. 1613–1621, 1997.

[11] D. Rörich, X. Wang, M. Bernhard, and J. Speidel, "Optimal Modulation Index of the Mach-Zehnder Modulator in a Coherent Optical OFDM System Employing Digital Predistortion," in *ITG Symposium on Photonic Networks*, vol. 9. Leipzig: VDE Verlag, 2013, pp. 95–100.

[12] M. Bernhard, D. Rörich, T. Handte, and J. Speidel, "Analytical and numerical studies of quantization effects in coherent optical OFDM transmission with 100 Gbit/s and beyond," in *ITG Symposium on Photonic Networks*. Leipzig: VDE Verlag, 2012, pp. 34–40.

[13] H. Bülow, W. Baumert, H. Schmuck, F. Mohr, T. Schulz, F. Küppers, and W. Weiershausen, "Measurement of the maximum speed of PMD fluctuation in installed field fiber," in *Optical Fiber Communication Conference*. Optical Society of America, 1999, pp. 83–85.

[14] P. Krummrich, E.-D. Schmidt, W. Weiershausen, and A. Mattheus, "Field trial results on statistics of fast polarization changes in long haul WDM transmission systems," in *Optical Fiber Communication Conference*, vol. 4. Optical Society of America, 2005, p. OThT6.

[15] W. Shieh and I. Djordjevic, *OFDM for Optical Communications*, 1st ed. Burlington: Elsevier, 2010.

[16] X. Yi, W. Shieh, and Y. Tang, "Phase estimation for coherent optical OFDM," *IEEE Photonics Technology Letters*, vol. 19, no. 12, pp. 919–921, Jun. 2007.

[17] S. D. Saliba, M. Junker, L. D. Turner, and R. E. Scholten, "Mode stability of external cavity diode lasers." *Applied optics*, vol. 48, pp. 6692–6700, 2009.

[18] W. Shieh, "Maximum-likelihood phase and channel estimation for coherent optical OFDM," *IEEE Photonics Technology Letters*, vol. 20, no. 8, pp. 605–607, Apr. 2008.

[19] X. Hong, X. Hong, and S. He, "Linearly interpolated sub-symbol optical phase noise suppression in CO-OFDM system," *Optics Express*, vol. 23, no. 4, p. 4691, 2015.